JOURNAL OF CATALYSIS 83, 107–120 (1983)

The Kinetics of H_2 Adsorption on and Desorption from Cobalt and the Effects of Support Thereon

JOHN M. ZOWTIAK AND CALVIN H. BARTHOLOMEW

BYU Catalysis Laboratory, Department of Chemical Engineering, Brigham Young University, Provo, Utah

Received November 30, 1982; revised April 14, 1983

The technique of temperature-programmed desorption (TPD) was applied to the investigation of hydrogen adsorption/desorption from a series of cobalt catalysts. Experiments in which the adsorption temperature was varied revealed that hydrogen adsorption on cobalt is activated and that the activation energy for adsorption is a function of catalyst support and metal loading. The activation energy for adsorption ranged from 5.8 kJ/mol for unsupported cobalt to 43 kJ/mol for 3% cobalt on silica. Desorption runs on selected catalysts showed hydrogen desorption to be second order, the heat of adsorption ranging from 145 kJ/mol on 10% Co/SiO_2 to 105 kJ/mol on 10% Co/Al_2O_3. Desorption from unsupported, silica-, and alumina-supported catalysts involved one major peak suggesting the presence of only one type of site while the titania- and carbon-supported catalysts displayed multiple desorption peaks providing evidence of a more complex distribution of surface sites possibly as a result of metal–support interactions. No H_2 adsorption was detected for magnesia-, ZSM-5, and lower loading (1 and 3%) alumina-supported cobalt catalysts at any temperature using flow adsorption/desorption techniques, even though these catalyst adsorbed hydrogen at temperatures ranging from 25 to 150°C using the static, equilibrium technique. These results suggest that strong metal–support interactions in these catalysts may lead to a strongly activated adsorption of hydrogen on cobalt.

INTRODUCTION

Temperature-programmed desorption (TPD), first applied to supported catalyst studies by Amenomiya and Cvetanovic (*1–3*) in 1963, has proven to be an increasingly powerful tool for the investigation of adsorption/desorption kinetics (*4–7*). Much of the earlier TPD work with supported metals was summarized in a recent review by Falconer and Schwartz (*7*).

At the time this study was undertaken, surprisingly little had been done to study the kinetics of desorption of important gases such as H_2 and CO from supported metals. Most of the previous work (*7*) had focused on TPD of H_2 and CO from platinum and nickel catalysts. Thus there was clearly a need for TPD studies of H_2 and CO from other important catalytic metals such as cobalt, iron, and ruthenium.

The present study of cobalt catalysts was undertaken as part of a more comprehensive investigation of cobalt–support interactions (*8–10*). Since there had been relatively few previous quantitative studies of hydrogen adsorption on cobalt (*11–14*), i.e., only three previous TPD studies of hydrogen desorption (*12–14*), one calorimetric study (*11*), and one surface potential study (*13*), this investigation included measurement of desorption kinetics of H_2 from unsupported and supported cobalt catalysts to determine the effects of support on adsorption states and energetics. The phenomenon of activated H_2 adsorption on cobalt was discussed in a previous communication from our laboratory (*9*). This paper reports quantitative kinetics for activated hydrogen adsorption on and desorption from cobalt in unsupported form and supported on Al_2O_3, SiO_2, TiO_2, and carbon.

EXPERIMENTAL

Materials. All gases used were ultra high purity grade (99.9995%) from Linde or Matheson. Hydrogen gas was further puri-

0021-9517/83 $3.00

fied with a Pt/Pd oxygen-removal catalyst (Girdler Catalysts, Chemetron Corp.) and a molecular sieve (Linde Type 5A). The carrier gas, nitrogen, was purified successively over a molecular sieve, a heated copper deoxo, another molecular sieve, and a Matheson Gas Purifier (Model 6406).

The adsorbate gas consisted of 10% hydrogen in nitrogen which was purified by passing over a Pt/Pd oxygen-removal catalyst followed by a molecular sieve trap. All gas flow rates were monitored at the exit of the system with a bubble flow meter and the flow rate was maintained between 20 and 40 cm^3/min for each catalyst run depending on catalyst loading.

Catalysts used in this study, methods of preparation, support properties, total H_2 uptakes, extents of reduction, and dispersions are summarized in Table 1. Details of the static H_2 adsorption and extents of reduction measurements are reported elsewhere (*8, 10*). The unsupported catalyst was prepared by overnight calcination of cobalt nitrate salt at 200°C followed by reduction for 16 hr at 400°C. The carbon-supported catalysts were prepared by evaporative deposition of a four to one mixture of benzene–ethanol which contained the support and the nitrate salt (*10*). The evaporation occurred under vacuum and constant stirring until dryness was obtained. All other catalysts were prepared by impregnation to incipient wetness of finely divided supports with cobalt nitrate solutions (*10*).

Procedure. All of the impregnated, supported catalysts were dried 12 hr at 100°C prior to reduction. To prevent the formation of cobalt–aluminates, the alumina-supported catalysts were reduced at 375°C for 16 hr while all other catalysts were reduced at 400°C for 16 hr. The reduction schedule

TABLE 1

Preparation and Properties of Cobalt Catalysts

Catalyst	Method of preparation[a]	Support type/supplier	Total H_2 uptake (μmol/g)[b]	Percentage redn[c]	Percentage D[d]
Unsupported cobalt	Thermal decomposition of $Co(NO_3)_2$	—	22	100	0.3
3% Co/SiO_2	Impregnation	Cab-O-Sil M-5	20	75	11
10% Co/SiO_2	Impregnation	(Cabot Corp)	82	92	10
1% Co/Al_2O_3	Impregnation	γ-Al_2O_3	3.2	11	34
3% Co/Al_2O_3	Impregnation	Dispal-M	5.6	22	10
10% Co/Al_2O_3	Impregnation	(Conoco)	29	34	9.9
15% Co/Al_2O_3	Impregnation		37	44	6.6
3% Co/TiO_2	Impregnation	P-25	4.5	14	17
10% Co/TiO_2	Impregnation	(Degussa)	17	47	4.5
3% Co/MgO	Impregnation	Dart Catalyst	0.6	11	2.1
10% Co/MgO	Impregnation	Division	2.1	13	1.9
3% Co/carbon	Evap. dep.	Type U U	18	13	55
10% Co/carbon	Evap. dep.	(Barnebey-Cheney)	143	47	36
3% Co/ZSM-5	Impregnation		0.4	NA[e]	—
9% Co/ZSM-5	Impregnation		11.2	NA	—

[a] All catalysts were dried at 100°C and reduced at 400°C for 16 hr.

[b] Total hydrogen uptake from static adsorption measurements at temperature of maximum adsorption (*10*).

[c] Percentage of cobalt reduced to the metal determined by O_2 titration of the reduced catalyst at 400°C and assuming formation of Co_3O_4 (*10*).

[d] Percentage dispersion (i.e., percentage exposed to the surface) calculated from $\%D = 1.179X/Wf$ where X = total H_2 uptake, W = wt% cobalt, f = fraction of cobalt reduced to the metal (*10*).

[e] NA, Not available.

included a temperature ramp of 3°C/min (from room temperature) with half hour holds at 100°C to facilitate water removal and at 200°C to ensure controlled nitrate decomposition.

The reactor consisted of a 0.64-cm-o.d. quartz tube surrounded by a 1.11-cm-diameter nichrome–wire-wrapped quartz tube furnace. A thermocouple placed in the annulus between the quartz tubes served to drive the temperature ramp while a thermocouple placed directly in the catalyst bed was used to continuously monitor catalyst temperature. Both thermocouples were chromel-alumel.

Temperature ramps from 1 to 100°C/min were delivered by an in-house-built temperature programmer. All desorption runs were carried out at 33°C/min. Adsorbate gas was injected into the carrier stream with a Carle six-port gas sampling valve (#5618) with a 0.1-cm^3 sample loop and which was controlled by a Carle Valve Minder II.

Desorbing hydrogen was detected with an HP Gas Chromatograph (Model 5730 A) equipped with a thermal conductivity detector (TCD). Before entering the cell, the carrier gas was split into two streams, one of which was routed to the reference cell and the other of which was passed through the sampling valve and reactor before entering the detector cell. To minimize time delay and pulse spreading effects, the chromatograph was operated without a column in place. The TCD was by-passed during reduction and operated at 110°C at all times to prevent the collection of any condensables. The TC signal was fed from the chromatograph to one channel of a Houston Instrument Omniscribe two pen recorder; the other channel carried the simultaneous signal from the thermocouple in the catalyst bed. The TCD analysis of H_2 was checked by two methods: (i) experiments in which no hydrogen was adsorbed on catalysts resulted in no TC signal and (ii) spectra for selected catalysts were reproduced well using a mass spectrometer detector; only H_2 was detected by the mass spectrometer. Baseline drift was reproducible and was corrected for in the subsequent analysis of the data.

Catalyst samples of from 30 to 100 mg (depending on cobalt loading and/or H_2 uptake) were reduced *in situ*. The typical procedure for adsorbing hydrogen on the surface was as follows. After reduction, the catalyst was cooled to room temperature in H_2, exposed to the carrier gas, temperature programmed to 400°C to desorb the H_2, and exposed to hydrogen once more. This cycle was repeated until reproducible desorption curves were obtained. Finally the catalyst was purged with carrier gas at 400°C, cooled to the adsorption temperature, after which 10% H_2/N_2 was pulsed onto the catalyst. Two kinds of TPD experiments were conducted. First, measurements of the quantity of hydrogen adsorbed at saturation were carried out for each catalyst as a function of adsorption temperature to obtain kinetic data for the activated adsorption and to determine the optimal temperature for conducting coverage-dependent investigations. Second, at the temperature of maximum adsorption, kinetics of desorption were obtained for each 10% catalyst as a function of coverage by varying the number of pulses of adsorbate.

In the course of the desorption rate versus coverage experiments it was determined that the manner in which H_2 was adsorbed on the catalyst influenced in a subtle but nevertheless significant way the peak shapes and desorption kinetics. It was found that "equilibrating" the adsorbed H_2 for 10–15 min in the carrier gas stream served to distribute the adsorbate more uniformly and resulted in uniform desorption kinetic orders over a wide range of coverage. Accordingly, all coverage-dependent desorption experiments were performed following this "equilibration" treatment.

The absence of pore diffusional effects, sample measurement lag time, and concentration gradients within each catalyst particle during the desorption rate measure-

ments was established according to the criteria of Gorte (*15*). Concentration gradients in the relatively thin beds (2–10 mm) were small as indicated by a lower than unity value ($<10^{-2}$) of the rate of H_2 desorption relative to the rate of flow leaving the cell. That is, since the instantaneous addition of H_2 to the gas phase at the front, middle, or any other part of the bed was slow relative to the gas flow out of the cell, it follows that the concentration gradient across the bed was small (less than 1%) at any instant during the experiment. Further evidence of small concentration gradients was that the peak temperature was relatively independent of flow rate under the conditions of this study.

RESULTS

Data Obtained by Varying Adsorption Temperature

Figures 1–5 show the family of H_2 desorption curves obtained for unsupported cobalt and 10% cobalt supported on SiO_2, Al_2O_3, TiO_2, and C as a function of adsorption temperature. The temperature at which maximum adsorption occurs, the peak desorption temperature corresponding to this maximum area, and the ratio of the maximum area to that at 25°C are listed in Table 2 for each of the catalysts investigated. The results for any given catalyst sample could be reproduced simply by repeating the adsorption/desorption cycle, a behavior indicating that the varying uptakes were not attributable to further reduction of the metal or other effects such as sintering etc. The area under each of these curves corresponds to saturation coverage for a given adsorption temperature. The temperature

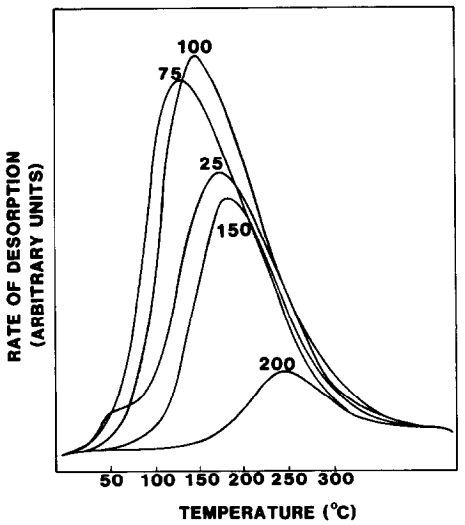

FIG. 1. H_2 TPD spectra for unsupported cobalt as a function of adsorption temperature.

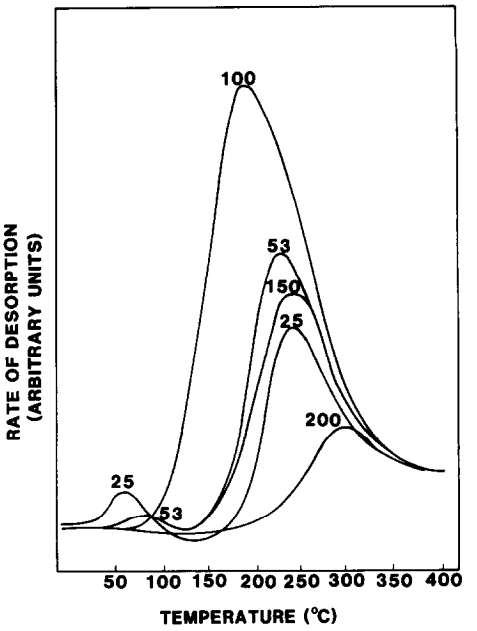

FIG. 2. H_2 TPD spectra for 10% Co/SiO_2 as a function of adsorption temperature.

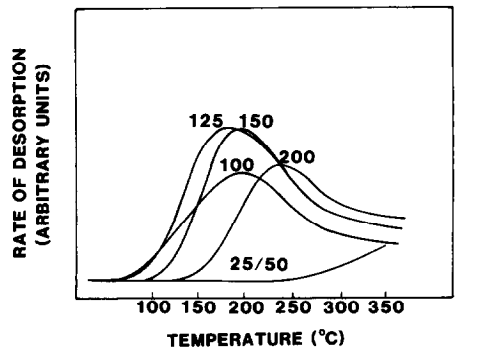

FIG. 3. H_2 TPD spectra for 10% Co/Al_2O_3 as a function of adsorption temperature.

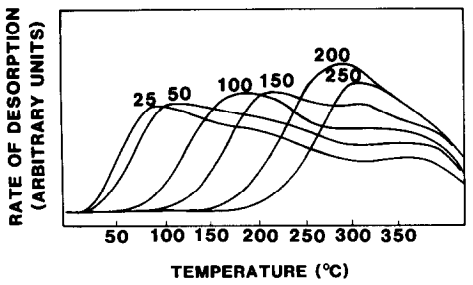

FIG. 4. H_2 TPD spectra for 10% Co/TiO_2 as a function of adsorption temperature.

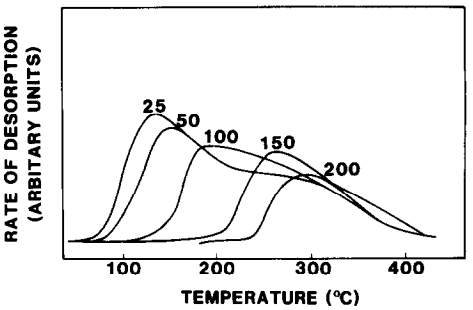

FIG. 5. H_2 TPD spectra for 10% Co/carbon as a function of adsorption temperature.

for maximum saturation coverage occurs significantly above room temperature for most of these catalysts (see Figs. 1–5 and Table 2), i.e., the adsorption is clearly activated. For example, the maximum adsorption of H_2 occurs on unsupported cobalt, Co/SiO_2, and Co/Al_2O_3 catalysts in the range of 100–150°C. Moreover, the temperature of this maximum adsorption appears to increase with increasing metal–support interaction (e.g., is 100 for unsupported cobalt and 10% Co/SiO_2, 125°C for 10% Co/Al_2O_3) and with decreasing metal loading

TABLE 2

Temperatures for Maximum Desorption of H_2, Peak Temperatures at Maximum Adsorption, and Areas at Maximum Adsorption Relative to Areas at 25°C for Cobalt Catalysts

Catalyst	Adsorption temperature (°C) for maximum uptake	Peak desorption temperature at maximum uptake (°C)	Area max/area 25°C	Maximum H_2 uptake[d] (μmol/g)
Unsupported	100	146	1.3	5.8
3% Co/SiO_2	150	188	33.5	—
10% Co/SiO_2	100	192	2.8	28
1% Co/Al_2O_3	No detectable uptake any temperature			0
3% Co/Al_2O_3	No detectable uptake any temperature			0
10% Co/Al_2O_3	125	183	[a]	19
15% Co/Al_2O_3	125	172	[a]	—
3% Co/carbon[b]	[c]	[c]	[c]	—
10% Co/carbon[b]	150	260	[c]	—
3% Co/TiO_2[b]	[c]	[c]	[c]	—
10% Co/TiO_2[b]	200	285	[c]	—
3% Co/MgO	No detectable uptake any temperature	—	—	0
10% Co/MgO	No detectable uptake any temperature	—	—	0
3% Co/ZSM-5	No detectable uptake any temperature	—	—	0
10% Co/ZSM-5		—	—	0

[a] No detectable uptake for these catalysts at room temperature—ratio essentially infinite.

[b] Multiple and overlapping desorption peaks. Data are reported for the highest temperature peak at maximum uptake.

[c] Data could not be determined for any single peak due to the presence of multiple overlapping desorption peaks.

[d] Determined by desorption after pulse-flow adsorption at the temperature of maximum uptake.

(e.g., is 100°C for 10% Co/SiO_2, 150°C for 3% Co/SiO_2).

Hydrogen adsorption on Co/TiO_2 at lower temperatures leads to TPD spectra involving 2 or more desorption peaks (see Fig. 4). The maximum area under the TPD curves is obtained after adsorption at 25°C; in other words H_2 adsorption does not appear to be activated based on the total spectrum area. However, the area under the low-temperature peak(s) decreases while the area under the high-temperature peak increases with increasing adsorption temperature. Thus adsorption on the sites of higher binding energy is activated. Similar behavior is observed for Co/C (Fig. 5). In the case of the lower loading (1 and 3%) Co/Al_2O_3 catalysts as well as 3 and 10% Co/MgO and 3 and 10% Co/ZSM-5 catalysts the support effect was dramatic, as there was no detectable hydrogen uptake observed (within our limits of detectability of about 50 nmol of H_2 or 0.5 μmol/g catalyst) at any temperature by TPD even when relatively large catalyst samples were employed, despite the fact that measurable H_2 uptake was observed for these same catalysts when the static, equilibrium method was employed (see Table 1).

Activation energies for adsorption (E_{Aa}) were obtained for unsupported, silica-supported, and alumina-supported cobalt catalysts according to the method of Schwartz *et al.* (*7, 16*) utilizing the following surface phase mass balance equation (*17*):

$$\theta_n/(1 - \theta_n) \cong \nu_a n u^{-1} \exp[-E_{Aa}/RT_a] \quad (1)$$

where u is the carrier gas flow rate, ν_a is the frequency factor for adsorption, and θ_n is the fractional coverage after adsorption of n equal size pulses at a given temperature T_a. Since the adsorption experiments were carried out at different temperatures but at a fixed flow rate and a fixed number of pulses, u, n, and ν_a were assumed to be constant. Values of θ_n were calculated from the areas under the TPD curves (e.g., Figs. 1–3) at temperatures ranging from 25°C to the maximum adsorption temperature. Values of θ_n were defined with respect to the monolayer adsorption obtained in static measurements (*10*). Activation energies for adsorption (E_{Aa}) were obtained from Arrhenius plots based on Eq. (1), i.e., $\ln [\theta_n/(1 - \theta_n)]$ versus $1/T_a$. This analysis assumed that the desorption rate was small relative to the adsorption rate at low adsorption temperatures. Indeed, no desorption was observed during these experiments. It also assumed that adsorption occurred uniformly through the catalyst bed and that the reaction order of adsorption was 2. Finally, it was assumed that E_{Aa} is independent of coverage.

Values of E_{Aa} are listed in Table 3 (second column). The activation energy for adsorption increases in the order unsupported, silica-supported, and alumina-supported cobalt; it is larger for 3% Co/SiO_2 compared to 10% Co/SiO_2.

Data Obtained by Varying Initial Coverage

From the adsorption versus temperature runs on each catalyst a temperature was chosen at which to carry out the coverage-dependent runs. This was usually the temperature of maximum adsorption. In the case of Co (unsupported), Co/SiO_2, and Co/Al_2O_3 this temperature was sufficiently elevated to minimize the interference of low temperature peaks. In the case of the titania- and carbon-supported catalysts multiple desorption peaks were observed (see Figs. 4 and 5) none of which could be adequately isolated for coverage dependent runs. Surface areas of 3% Co/SiO_2 and Co/Al_2O_3 were too low for measurement of quantitative desorption kinetics. Consequently coverage dependent runs were conducted on the unsupported cobalt, 10% Co/SiO_2, and 10% Co/Al_2O_3 catalysts only.

Each catalyst was raised to the preselected temperature, exposed to a predetermined amounts of hydrogen, allowed to equilibrate (in the flowing carrier gas) for 5 mins, cooled to room temperature, after which a temperature-programmed desorption was carried out. A family of desorption

TABLE 3

Activation Energies and Heats of Adsorption and Desorption for H_2/Cobalt

Catalyst	E_{Aa} (kJ/mol)[a]	E_{Ad} (kJ/mol)[b]	$-\Delta H_a$[c]	Order of desorption	Reference
This study					
Unsupported Co	5.8	151	145 ± 10	2	This work
3% Co/SiO_2	43		—	—	This work
10% Co/SiO_2	18	168	145 ± 7	2	This work
10% Co/Al_2O_3	39	144	105	2	This work
Previous studies					
Reduced Co (Calorimetric)			105		*11*
Co/Rutile		88/138			*12*
Co Films (Surface Pot./TPD)		42/79			*13*
Single Crystal Co (0001)		67		2	*14*

[a] Activation energy for adsorption of H_2.
[b] Activation energy for desorption of H_2.
[c] Heat of adsorption, $-\Delta H_a = E_{Ad} - E_{Aa}$.

rate versus temperature curves at different initial coverages was obtained for each catalyst studied, an example of which is shown for unsupported cobalt in Fig. 6. Fractional initial coverage θ was defined in this study, as in the studies of previous workers (*5, 16*), as the ratio of the total area under the TPD curve at less than maximum coverage to the total area under the curve at maximum (saturation) coverage for a given adsorption temperature.

Kinetics of desorption were analyzed using the desorption rate isotherm method (*5, 7, 16*). Plots of ln [desorption rate] versus ln $[\theta/(1-\theta)]$ were made at several temperatures to obtain values for the order of desorption. This treatment was based on the assumptions that adsorption occurs according to Langmuir kinetics, readsorption occurs freely, the reaction order of adsorption is equal to that for desorption, and the reactor can be treated as a differential-bed. Plots of ln (rate) vs ln $[\theta/1-\theta]$ for unsupported cobalt, 10% Co/SiO_2, and 10% Co/Al_2O_3 are shown in Figs. 7–9. From the slopes of the lines in Figs. 7–9 the desorption order was found to be 2 over reasonably wide ranges of temperature (and coverage), although there were significant variations in the slopes (i.e., 1.2 to 2.6) at high and low temperatures of desorption. The lower values of the slope slightly above 1 were observed mainly at low temperatures and high coverages.

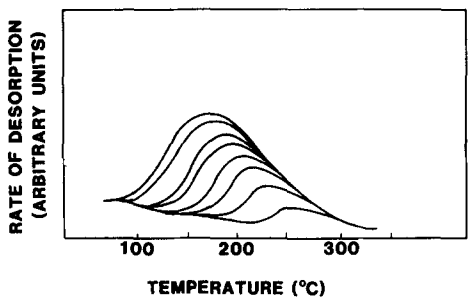

FIG. 6. H_2 desorption spectra for unsupported cobalt after adsorption at 100°C as a function of initial coverage.

From the plots of ln (rate) versus ln $[\theta/1-\theta]$ (e.g., Figs. 7–9) it is possible to obtain rate versus temperature data at fixed values of coverage. A typical Arrhenius plot of data obtained in this manner for 10% Co/Al_2O_3 is shown in Fig. 10. The enthalpies of adsorption obtained from these plots were extrapolated to zero coverage (see Figs. 11a,b,c) to obtain the values of ΔH_a listed in Table 3. The values of ΔH_a for unsupported cobalt and Co/SiO_2 were found to be in very close agreement (−145 kJ/mol in both

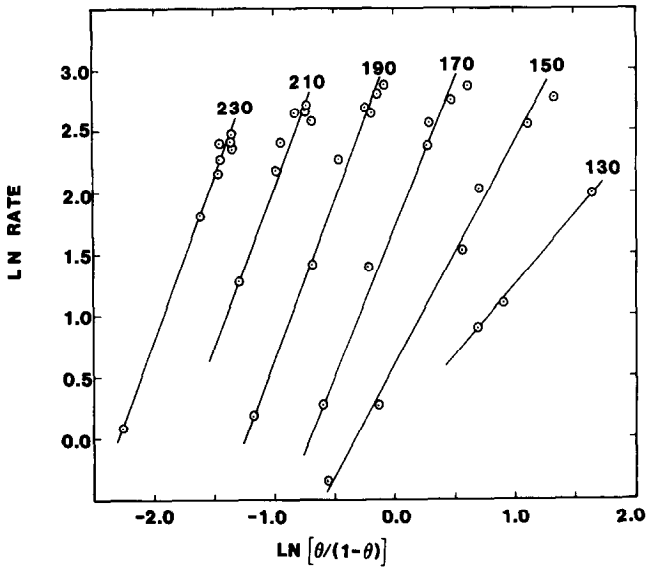

FIG. 7. ln [desorption rate] versus ln $[\theta/(1-\theta)]$ for hydrogen desorption from unsupported cobalt. Each line corresponds to a different desorption temperature (in °C).

cases) while that for Co/Al_2O_3 (−105 kJ/mol) was determined to be significantly (33%) less negative. Since $-\Delta H_a = E_{ad} - E_{Aa}$ it is possible to calculate values of the activation energy for desorption E_{Ad} from the measured values of E_{Aa} and ΔH_a (see Table 3). Values of E_{Ad} were found to range from 144 for Co/Al_2O_3 to 168 for Co/SiO_2.

DISCUSSION

Kinetics of Hydrogen Adsorption on Cobalt

The adsorption versus temperature data in this study (Figs. 1–5 and Tables 2 and 3) provide quantitative evidence that adsorption of H_2 on cobalt is activated and that the extent of activation is a function of support

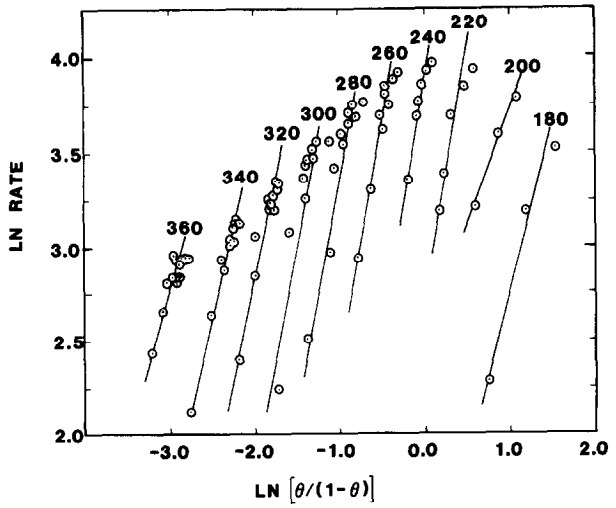

FIG. 8. ln [desorption rate] versus ln $[\theta/(1-\theta)]$ for hydrogen desorption from 10% Co/SiO_2. Each line corresponds to a different temp for desorption (in °C).

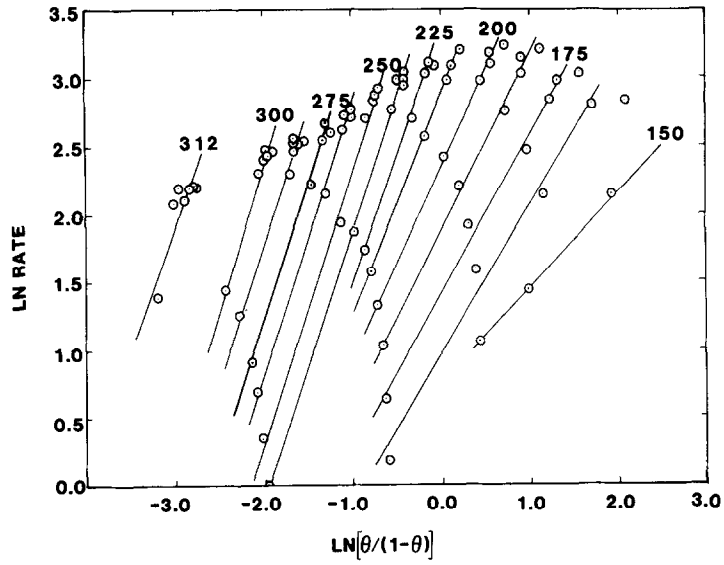

FIG. 9. ln [desorption rate] versus ln $[\theta/(1-\theta)]$ for hydrogen desorption from 10% Co/Al_2O_3. Each line corresponds to a different desorption temperature (in °C).

and metal loading. The phenomenon of activated H_2 adsorption on cobalt was observed in three previous investigations (*12, 18, 19*). Matsumura *et al.* (*18*) reported that H_2 adsorption on potassium-promoted cobalt was activated above 60°C and that maximum adsorption occurred at about 200°C. Sastri and Srinivasan (*19*) observed increasing H_2 adsorption with increasing temperature on a series of Co/Kieselguhr catalysts; the maximum H_2 adsorption occurred on these catalysts at about 50°C. Dollimore and Harrison (*12*) observed negligible adsorption of H_2 on Co/TiO_2 at 25°C, although significant H_2 adsorbed at 300°C.

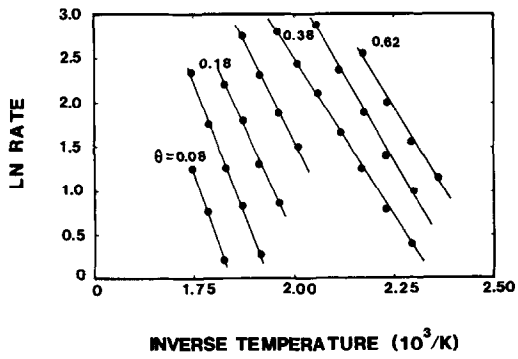

FIG. 10. Arrhenius plots for H_2 desorption from 10% Co/Al_2O_3 at different fractional coverages.

Although these previous studies (*12, 18, 19*) established that the quantity of hydrogen adsorbed on cobalt increases with increasing temperature, there were significant variations in the reported temperatures for maximum adsorption. The data in this study provide a basis for explaining the differences, i.e., *the extent of activation apparently changes with support and metal loading*. Moreover, this study is the first to report quantitative kinetic data, i.e., activation energies for adsorption of hydrogen on cobalt.

The fact that the activation energy for H_2 adsorption on cobalt increases in the order unsupported Co, Co/SiO_2, Co/Al_2O_3, and as the metal loading for Co/SiO_2 is decreased from 10 to 3% (see Table 3), suggests that the activation barrier for dissociative adsorption on cobalt increases with increasing degree of metal–support interaction. Previous investigations (*20–22*) have shown that metal–support interactions can result in suppression of H_2 and CO adsorption in Ni/Al_2O_3, Ni/TiO_2, and Pt/TiO_2 catalysts. Such phenomena have been interpreted as

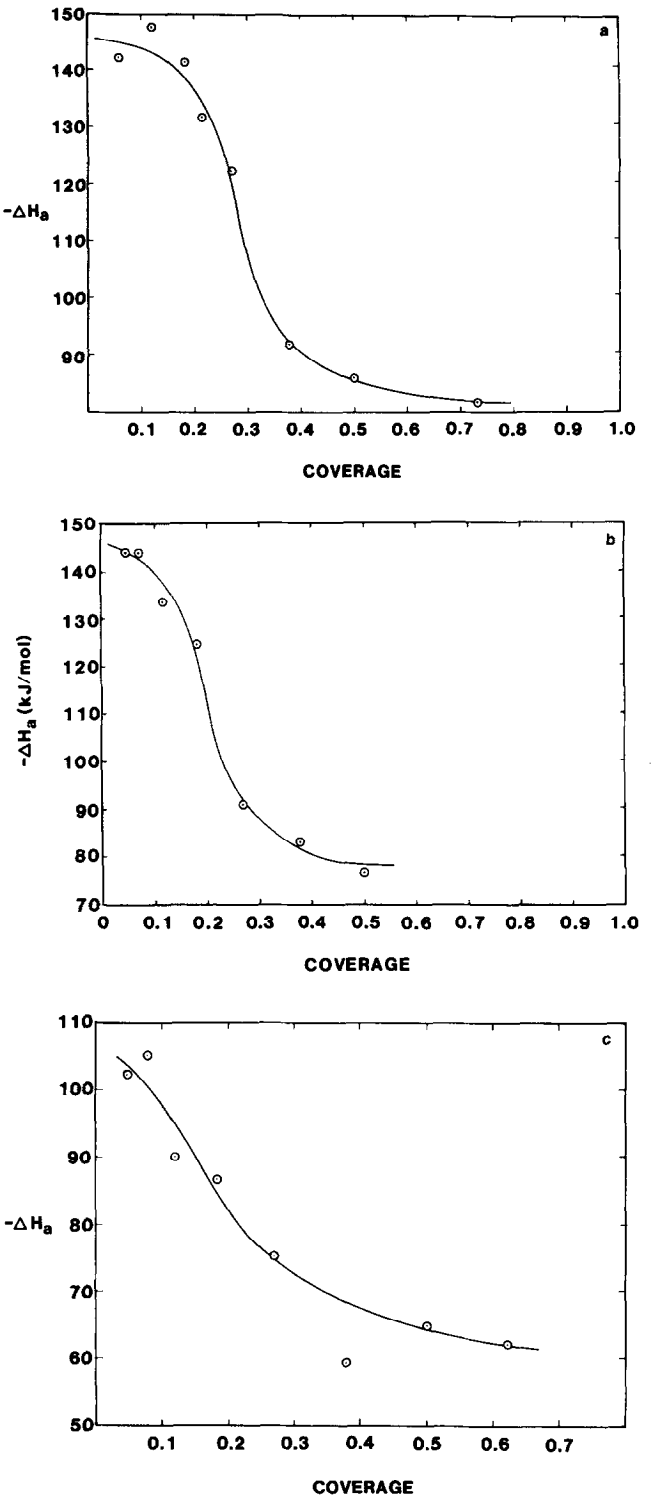

FIG. 11. (a) Enthalpy of adsorption of hydrogen on unsupported cobalt as a function of surface coverage. (b) Enthalpy of adsorption of hydrogen on 10% Co/SiO_2 as a function of surface coverage. (c) Enthalpy of adsorption of hydrogen on 10% Co/Al_2O_3 as a function of surface coverage.

evidence of an electronic interaction at the metal–oxide interface which changes the electronic properties of the metal (*23, 24*). The changes in activation energy for H_2 adsorption in this study provide further evidence of electronic modifications in the metal due to metal–support interactions.

Could the phenomenon of increasing H_2 adsorption with increasing temperature be a result of processes other than kinetically limited adsorption? Probably not, since the evidence heavily favors the kinetically limited adsorption process. First, the nature of the increasing adsorption with increasing temperature observed in this and previous studies (*12, 18, 19*) is very consistent with the concept and experimental observations of activated adsorption described by Taylor and others (*19, 25*). Second, the fact that in this study no measurable H_2 adsorption was observed on several cobalt catalysts using the pulse-adsorption technique while significant amounts chemisorbed using the static technique in which catalysts were equilibrated 45 min (*10*) provides further evidence of a kinetically limited adsorption process. The observed results are not due to phase transitions or to bulk absorption. Although cobalt undergoes a transition from a hexagonal to a cubic crystal structure in the temperature range 417–450°C (*26*), the experiments in this study were conducted at temperatures below 400°C and hence the transition was not a factor. Hydrogen absorption into bulk cobalt is insignificant compared to the hydrogen uptakes observed in this study even at elevated temperatures (*27*).

The observation that hydrogen adsorption on cobalt, especially supported cobalt, is strongly activated has important implications in regard to experimental practices for measuring hydrogen adsorption uptakes on cobalt catalysts. It is convention to use H_2 adsorption at room temperature to estimate metal dispersion, metal particle size, and specific reaction rates in the form of turnover frequencies (*28–33*). However, the data of this study show that significantly greater quantities of H_2 adsorb at higher temperature relative to room temperature (see Table 2), e.g., 30–50 times more H_2 on 3% Co/SiO_2 at 150°C and infinitely larger quantities of H_2 on 10% Co/Al_2O_3 at 125°C relative to 25°C using the pulse-adsorption technique. Moreover, recent studies in our laboratory (*10, 34*) reveal that significantly larger quantities of H_2 adsorb on 3–9% Co/ZSM-5 and 3% Co/Al_2O_3 at 100–125°C compared to 25°C using the static technique in which catalysts are equilibrated in 300–400 Torr H_2 for 45 min. Accordingly, previously reported dispersions (*29–31*) based on room temperature H_2 uptakes are probably erroneously low while reported turnover frequencies are erroneously high, particularly those measured for 2–5% Co/Al_2O_3 and Co/SiO_2 (*29, 30*). Furthermore the results of this study explain the unexpectedly low H_2 uptake of 1 μmol/g reported by Vannice for 2% Co/Al_2O_3 (*29*).

In view of the strongly activated adsorption of H_2 on cobalt, what are acceptable techniques for measuring monolayer coverage? There are essentially two alternatives: (i) measurement of the total H_2 uptake at the temperature of maximum adsorption, determined separately for each cobalt catalyst or (ii) measurement of the total uptake at 25°C after cooling in H_2 from the reduction temperature (e.g., 400–450°C) similar to the method proposed by Amelse *et al.* (*33*). This latter approach has the advantage of ensuring that maximum adsorption is obtained without requiring previous measurements of uptake versus temperature to determine the optimum. In using either alternative it should be emphasized that total monolayer coverage is best obtained using the static adsorption technique (*10, 35*), since the flow technique (*33*) measures only strongly held hydrogen and since a portion of the hydrogen monolayer on cobalt is reversibly adsorbed (*10*).

Kinetics of H_2 Desorption from Cobalt

The approach used in this study to determine desorption kinetics and heats of ad-

sorption was based on the following assumptions: (i) applicability of Langmuir kinetics, (ii) rapid readsorption, (iii) the same orders of reaction for adsorption and desorption, and (iv) differential behavior for the TPD reactor. These assumptions are justified as follows.

In their TPD investigation of H_2 desorption from Ni/SiO_2 Lee and Schwarz (*16*) demonstrated that Langmuir kinetics involving reaction orders of 2 with respect to unoccupied and occupied sites for adsorption and desorption provided a very good fit to their data. Bridge *et al.* (*14*) observed a desorption order of 2 for hydrogen desorption from Co (0001). Similarly in this study the data (Figs. 7–9) were most consistent with an order of desorption of 2 over wide ranges of coverage and temperature. Moreover, one would predict a priori that the dissociative adsorption and associative desorption of H_2 on metals should be second order in unoccupied sites and occupied sites, respectively, since adsorption requires two sites and desorption requires association of two hydrogen atoms. At low temperatures (high coverages) the slopes corresponded to lower values of n (e.g., $n = 1$), in agreement with the observations of Lee and Schwarz. This might be due to desorption of a molecularly adsorbed H_2, such as that proposed by Dus and Lisowski (*13*) or due to nonuniform adsorption of H_2.

The assumption of differential reactor behavior for the TPD reactor in this study was justified in view of the small quantities of catalyst used (30–100 mg) and the high flow rates (20 to 40 cm^3/min) relative to the rates of desorption. As in the study of Lee and Schwarz (*16*) the data were fitted in a consistent manner by assuming free readsorption. The fit of the data to the rate expression derived by neglecting readsorption was in comparison poor and resulted in inconsistent values for reaction orders, etc.

Based on the data from this study it appears that the heat of adsorption and hence the binding energy for hydrogen is the same within experimental error for unsupported and silica-supported cobalt but significantly lower for alumina-supported cobalt (see Table 3). This lowering of the binding energy for hydrogen with cobalt might occur as a result of a partial transfer of electrons from cobalt crystallites to the alumina support. This hypothesis might be checked experimentally through careful ESCA and/or Mössbauer effect measurements.

In comparing our data with those from previous TPD, surface potential, and calorimetric studies (see Table 3), it is apparent that our activation energies of desorption and heats of adsorption are generally higher, although the activation energy of desorption of 138 kJ/mol reported for the high temperature peak of Co/rutile (*12*) is close to the value reported in this study of 144 kJ/mol for Co/Al_2O_3. The lower values of E_{Ad} reported by other previous workers (*13, 14*) can be explained by (i) their failure to extrapolate their data to zero coverage (*13*) and/or (ii) kinetic limitations due to their adsorbing H_2 on their samples at low temperatures (*13, 14*). Since the calorimetric heat of 105 kJ/mol (*11*) was determined after adsorption at 20°C, like the TPD data on polycrystalline and single crystal cobalt (*13, 14*), it did not include the heat due to adsorption of H_2 on the more energetic sites. Indeed Rudham and Stone (*11*) observed a tendency for the incremental heat to increase with time during the period of measurement, which they attributed to a slower adsorption process associated with a higher heat. Unfortunately they did not measure this additional heat or the heat of adsorption at higher temperatures. Thus their reported value is representative of the less energetic sites only and would clearly be lower than that measured in this study after adsorption at higher temperatures.

It should be emphasized that the desorption rates and hence the heats of adsorption measured for H_2 on polycrystalline cobalt and supported cobalt in this study clearly represent averages of the contributions from sites of different coordination (i.e., different crystallographic planes). While

these data provide a measure of the kinetics and energetics of adsorption on cobalt catalysts, they may not provide an accurate measure of the behavior on various single crystal planes of cobalt, particularly if the binding energies of H_2 differ greatly from plane to plane. However, it is more likely that the binding energies of H_2 on different cobalt planes are relatively similar, since those for various planes of nickel vary by only 3–5 kJ/mol (*16, 36, 37*). That there has been only one previous study of H_2 desorption from single crystal cobalt (*14*) emphasizes the need for further surface science studies of hydrogen adsorption on well-defined cobalt.

It is interesting to compare the heat of adsorption of 145 kJ/mol obtained from this study for H_2 on 10% Co/SiO_2 with the values of 89 kJ/mol obtained for H_2 adsorption on 45% Ni/SiO_2 by Lee and Schwartz (*16*) and of 90 and 85 kJ/mol obtained for H_2 adsorption on 45 and 10% Ni/SiO_2 by Weatherbee and Bartholomew (*36*). This comparison indicates that H_2 is significantly more strongly adsorbed on cobalt relative to nickel, i.e., the heat of adsorption is 55–60 kJ/mol larger. This conclusion is consistent with a previous correlation of specific methanation activity for silica-supported metals versus heats of adsorption for CO on single crystals of Group VIII metals (*30*), in which Co/SiO_2 was considered to be most active because of its optimum heat of adsorption. However, the present study and previous studies of Ni/SiO_2 (*16, 36*) provide the basis for correlating ΔH_a values for H_2 on real silica-supported catalysts.

CONCLUSIONS

(1) Hydrogen adsorption on cobalt is activated, i.e., maximum adsorption occurs at temperatures significantly above 25°C.

(2) The extent of activation (i.e., activation energy for adsorption) is greatly influenced by the support. It appears to increase with increasing extent of metal–support interaction and decreasing metal loading.

(3) The concept of activated H_2 adsorption on cobalt has important implications for reaction and adsorption studies. Previously reported turnover numbers and metal surface areas for cobalt catalysts may be significantly in error. Previously measured heats of adsorption for H_2 on cobalt and activation energies for desorption of H_2 from cobalt may also be erroneously low, since the adsorption at 25°C was kinetically limited.

(4) Heats of adsorption for H_2 on cobalt are affected by the support. For example, the heat of adsorption of H_2 on Co/Al_2O_3 is 40 kJ/mol less than on Co/SiO_2 or unsupported Co. The heat of adsorption of H_2 on Co/SiO_2 is 55–60 kJ larger than for H_2 on Ni/SiO_2.

ACKNOWLEDGMENTS

The authors gratefully acknowledge financial support from the Department of Energy, Office of Basic Energy Sciences, Division of Chemical Sciences (Contract No. DE-AC02-81ER10855), technical assistance by Mr. Gordon D. Weatherbee and Mr. Robert Reuel, and valuable comments by Professors Douglas N. Bennion (Brigham Young University) and Raymond J. Gorte (University of Pennsylvania).

REFERENCES

1. Amenomiya, Y., and Cvetanovic, R. J., *J. Phys. Chem.* **67,** 144 (1963).
2. Cvetanovic, R. J., and Amenomiya, Y., *Adv. Catal.* **17,** 103 (1967).
3. Cvetanovic, R. J., and Amenomiya, Y., *Catal. Rev.* **6,** 21 (1972).
4. Schmidt, L. D., *Catal. Rev-Sci. Eng.* **9,** 115 (1974).
5. Falconer, J. L., and Madix, R. J., *J. Catal.* **48,** 262 (1977).
6. Ibok, E. E., and Ollis, D. F., *J. Catal.* **66,** 391 (1980).
7. Falconer, J. L., and Schwarz, J. A., *Catal. Rev-Sci. Eng.* **25,** 141 (1983).
8. Bartholomew, C. H., Reuel, R., and Zowtiak, J. M., Annual Report to DOE, DOE/ER/10855-1, April 30, 1982.
9. Zowtiak, J. M., and Bartholomew, C. H., *J. Catal.*, in press (1983).
10. Reuel, R., and Bartholomew, C. H., *J. Catal.*, submitted (1983).
11. Rudham, R., and Stone, F. S., *Trans. Faraday Soc.* **54,** 421 (1958).
12. Dollimore, J., and Harrison, B., *J. Catal.* **28,** 275 (1973).

13. Dus, R., and Lisowski, W., *Surface Sci.* **61,** 635 (1976).
14. Bridge, M. E., Comrie, C. M., and Lambert, R. M., *J. Catal.* **58,** 28 (1979).
15. Gorte, R. J., *J. Catal.* **75,** 164 (1982).
16. Lee, P. I., and Schwarz, J. A., *J. Catal.* **73,** 272 (1982).
17. Zowtiak, J. M., M. S. Thesis, Brigham Young University, 1983.
18. Matsumura, S., Tarama, K., and Kodama, S., *J. Soc. Chem. Ind. (Japan)* **43,** 175 (1940) Supplemental Binding.
19. Sastri, M. V. C., and Srinivasan, V., *J. Phys. Chem.* **59,** 503 (1955).
20. Tauster, S. J., Fung, S. C., and Garten, R. L., *J. Amer. Chem. Soc.* **100,** 170 (1978).
21. Vannice, M. A., and Garten, R. L., *J. Catal.* **56,** 236 (1979).
22. Bartholomew, C. H., Pannell, R. B., and Butler, J. L., *J. Catal.* **65,** 335 (1980).
23. Tauster, S. J., Fung, S. C., Baker, R. T. K., and Horsley, J. A., *Science* **211,** 1121 (1981).
24. Horsley, J. A., *J. Amer. Chem. Soc.* **101,** 2870 (1979).
25. Taylor, H. S., *J. Amer. Chem. Soc.* **53,** 578 (1931).
26. Young, R., "Cobalt: ACS Monograph Series 149." Reinhold, 1960.
27. Nichols, D., "Pergamon Texts in Inorganic Chemistry: Vol. 24, The Chemistry of Fe, Co, and Ni." Pergamon, Oxford, 1975.
28. Farrauto, R. J., *AIChE Symp. Ser.* **70,** 9 (1975).
29. Vannice, M. A., *J. Catal.* **37,** 449 (1975).
30. Vannice, M. A., *J. Catal.* **50,** 228 (1977).
31. Kibby, C. L., Pannell, R. B., and Kobylinski, T. P., Proceedings of the Seventh Canadian Symposium on Catalysis, Edmonton, Alberta, Oct. 19–22, 1980.
32. Arcuri, K. B., Butt, J. B., and Schwartz, L. H., presented at the Symposium on Multimetallic Catalysts, Div. of Colloid and Surface Chemistry, 183rd National Meeting of the ACS, March 28–April 2, Las Vegas, NV.
33. Amelse, J. A., Schwartz, L. M., and Butt, J. B., *J. Catal.* **72,** 95 (1981).
34. Bartholomew, C. H., Annual Technical Progress Report to DOE, DOE-ET-14809-8, October 31, 1981.
35. Bartholomew, C. H., and Pannell, R. B., *J. Catal.* **65,** 390 (1980).
36. Weatherbee, G. D., and Bartholomew, C. H., *J. Catal.*, submitted (1983).
37. Toyoshima, I., and Somorjai, G. A., *Catal., Rev.-Sci. Eng.* **19,** 105 (1979).